Guo B
Cardiff University
School of Engineering

Meng J
STFC Daresbury Laboratory
Scientific Computing Department

Pan S
Cardiff University
School of Engineering

Ning D
Dalian University of Technology
State Key Laboratory of Coastal and Offshore Engineering

SUSTAINABLE ENERGY

Numerical Wave Flume with Lattice Boltzmann Method for Wave Energy Converters

Based on Lattice Boltzmann Method, a free interface tracking model using volume of fraction (VOF) technique is built to explore the interaction of Oscillating Water Column (OWC) type of Wave Energy Converters (WECs) with waves. In the numerical wave flume, the momentum source is applied to generate incident waves and absorb reflected waves. After validation, one stationary OWC in the absence of Power take-off system (PTO) is then placed in the numerical wave flume to examine the performance of the numerical scheme. The simulation results show that the numerical stability is well achieved with the wave-structure interaction included and there is a strong vortex shedding at wall corner and nonlinearity with smaller amplitude in the present viscous flow model, compared with the linear potential flow solution.

Keywords:
Lattice Boltzmann method, numerical wave flume, wave-structure interaction, oscillating water column, wave energy converters.

Corresponding author:
GuoB5@cardiff.ac.uk

B. Guo, S. Pan, J. Meng, and D. Ning, 'Numerical Wave Flume with Lattice Boltzmann Method for Wave Energy Converters', *Proceedings of the Cardiff University Engineering Research Conference 2023*, Cardiff, UK, pp. 168-172.

doi.org/10.18573/conf1.al

INTRODUCTION

The wave energy capture efficiency (CWR) is indeed overestimated in the theoretical potential flow model developed. To study the hydrodynamic effects of viscosity and nonlinearity, a numerical wave flume is created using the Lattice Boltzmann method (LBM) to investigate the wave-OWC interaction. The LBM method possesses high expansibility on the parallel computing for the outstanding locality and stability, which can comparably improve the simulation efficiency on solving a viscous flow problem [1, 2].

MATERIALS AND METHODS

The present model uses MRT-LBM method to solve N-S equation, in which VOF-based free-surface capturing technique by Korner et al. [3] is adopted. Wave is generated by the momentum source and absorbed by the sponge layer [4], as shown in Fig.1. These algorithms are implemented using the High Level Mesoscale System [5].

Lattice Boltzmann method

Boltzmann equation describes the evolution of the density distribution function $f_\alpha(x,t)$. Its general form with the forcing term in the MRT (Multi-Relaxation-Time) model can be written as follows:

$$f_\alpha(\boldsymbol{x}+\boldsymbol{e}_\alpha\delta t, t+\delta t) - f_\alpha(\boldsymbol{x},t) = -\boldsymbol{M}^{-1}[\boldsymbol{S}(\boldsymbol{m}-\boldsymbol{m}^{eq})] + \boldsymbol{M}^{-1}\boldsymbol{\Phi}\delta t \quad (1)$$

where $\boldsymbol{x}$ is the spatial position and t is the time; $\boldsymbol{e}_\alpha$ is the discrete velocity; δt is the non-dimensional time step and non-dimensional grid spacing $\delta x = \delta t \cdot \sqrt{3}$; α ranges from 1 to 9 in two-dimensional space; $\boldsymbol{M}$ and $\boldsymbol{S}$ are transformation matrix and relaxation matrix, respectively. $\boldsymbol{\Phi} = \boldsymbol{M}\overline{\boldsymbol{F}}$ is the forcing term in moment space, where the Guo Forcing Scheme is applied here:

$$\boldsymbol{\Phi} = \left(\boldsymbol{I} - \frac{\boldsymbol{S}}{2}\right)\delta t\left(0, 6(\boldsymbol{F}\cdot\boldsymbol{u}), -6(\boldsymbol{F}\cdot\boldsymbol{u}), F_x, -F_x, F_y, -F_y, 2(F_x u_x - F_y u_y), F_y u_x + F_x u_y\right)^T \quad (2)$$

Then the macroscopic quantities can be calculated by the velocity moments,

$$\rho = \sum_\alpha f_\alpha \,,\ \rho_0 \boldsymbol{u} = \sum_\alpha \boldsymbol{e}_\alpha f_\alpha + \frac{\boldsymbol{F}}{2}\delta t \quad (3)$$

Free-surface capturing method

Following Korner et al. [3], the single-phase VOF (volume of fluid) method is used to capture the gas-liquid interface. The fill level of each discrete cell with fluid is evaluated by the volume fraction,

$$\varepsilon = \frac{V_{fluid}}{V_{cell}} \quad (4)$$

It is clear that $\varepsilon = 0$ means the present cell is an empty cell and $\varepsilon = 1$ corresponds to a fill cell. The all interface cells with $0 < \varepsilon < 1$ separate liquid from gas. The fill level can be further expressed as,

$$\varepsilon = \frac{m_{fluid}}{\rho_{fluid}} \quad (5)$$

In the standard VOF-LBM model, we adopt the first-order explicit Euler time difference scheme,

$$m(\boldsymbol{x}, t+\delta t) = m(\boldsymbol{x},t) + \sum_\alpha \Delta m_\alpha \quad (6)$$

The mass exchange Δm_α, associated with the convective term, between an interface cell at lattice node x and its neighbor at $\boldsymbol{x} + \boldsymbol{e}_\alpha\delta t$ is calculated as,

$$\Delta m_\alpha(\boldsymbol{x},t) = \left(f_{\bar{\alpha}}(\boldsymbol{x}+\boldsymbol{e}_\alpha\delta t, t) - f_\alpha(\boldsymbol{x},t)\right) A_\alpha$$
$$A_\alpha = \begin{cases} 0, & neighbor\ is\ empty\ cell \\ \dfrac{\varepsilon(\boldsymbol{x},t) + \varepsilon(\boldsymbol{x}+\boldsymbol{e}_\alpha\delta t, t)}{2}, & neighbor\ is\ interface\ cell \\ 1, & neighbor\ is\ fluid\ cell \end{cases} \quad (7)$$

where $\boldsymbol{e}_{\bar{\alpha}} = -\boldsymbol{e}_\alpha$.

Once the mass exchange has been evaluated, the VOF of each cell ε can be updated on Eq.5. In the advection step, the interface cells may be emptied or filled, corresponding to $\varepsilon < 0$ and $\varepsilon < 1$ respectively. For those interface cells, their state needs to be updated: the emptied cell to empty cell and the filled cell to fluid cell. To seal the gas-liquid interface, the surrounding empty cells at each filled cell must be converted to interface cells and surrounding fluid cells at each emptied cell must be converted to interface cells. Then, since there is no valid information at each gas cell (empty cell) in the present single-phase flow model, those new interface cells converted from empty cells needs to be initialized with equilibrium distribution $f_\alpha^{\mathrm{eq}}(\rho^{\mathrm{avg}}, u^{\mathrm{avg}})$, in which the macroscopic quantities ρ^{avg} and u^{avg} are obtained from the average values of the surrounding fluid and interface cells at the moment $t + \delta t$.

Moreover, the mass conservation is required in the advection. That is to say, the excess mass from emptied $\varepsilon < 0$ and filled $\varepsilon < 1$ cells needs to be distributed to the neighbouring interface cells as,

$$m(\boldsymbol{x}+\boldsymbol{e}_\alpha\delta t) = m(\boldsymbol{x}+\boldsymbol{e}_\alpha\delta t) + m^{ex}\frac{\nu_\alpha}{\nu_{total}} \quad (8)$$

where excess mass $m^{\mathrm{ex}} = \rho$ for the emptied cells and $m^{\mathrm{ex}} = m - \rho$ for the filled cells.

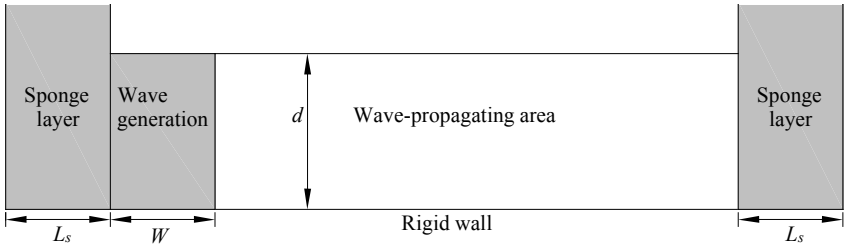

Fig. 1. Sketch of the numerical wave flume

Boundary conditions
For no-slip boundary conditions, a halfway bounce back scheme is used, the incoming unknown density distribution $f_{\bar{\alpha}}$ is reconstructed as,

$$f_{\bar{\alpha}}(\boldsymbol{x}, t+\delta t) = f_{\alpha}^{out}(\boldsymbol{x}, t) \tag{9}$$

Here $f_{\alpha}^{\mathrm{out}}$ denotes the density distribution function after the collision step. At the slip boundary, the bounce forward scheme is adopted to reconstruct the missing distribution,

$$f_{\alpha^*}(\boldsymbol{x}, t+\delta t) = f_{\alpha}^{out}(\boldsymbol{x} - \boldsymbol{e}_{\alpha}\boldsymbol{t}\delta t, t) \tag{10}$$

where α^* is the mirrored direction to α with $\boldsymbol{e}_{\alpha^*}\boldsymbol{t} = \boldsymbol{e}_{\alpha}\boldsymbol{t}$ and $\boldsymbol{e}_{\alpha^*}\boldsymbol{n} = -\boldsymbol{e}_{\alpha}\boldsymbol{n}$ (wall normal direction $\boldsymbol{n}$ and tangential direction $\boldsymbol{t}$).

At a free surface boundary, it is obvious that the incoming distributions from empty cells are unknown as the dynamics of gas phase does not be considered in the present single-phase flow model. Therefore, the free surface kinetic boundary condition (FSK) proposed by Korner et al. [3] is applied here to reconstruct those missing distributions,

$$f_{\bar{\alpha}}(\boldsymbol{x}, t+\delta t) = -f_{\alpha}^{out}(\boldsymbol{x}, t) + f_{\alpha}^{eq}\big(\rho_A, \boldsymbol{u}(\boldsymbol{x}, t)\big) + f_{\bar{\alpha}}^{eq}\big(\rho_A, \boldsymbol{u}(\boldsymbol{x}, t)\big) \tag{11}$$

where $\rho_{\mathrm{A}} = p_{\mathrm{A}}$ in present LBM unit system is related to surrounding atmosphere pressure.

Smagorinsky LES
Free surface flows are characterized by high Reynolds numbers in the turbulent regime. Therefore, a large eddy model is used to simulate turbulent flows in the case of limited computing resource. The LBE-LES model is introduced in which the eddy viscosity ν_t is [2],

$$\nu_t = (C_s \delta x)^2 \|\bar{\boldsymbol{S}}\| \tag{12}$$

where C_s is the Smagorinsky constant, and mean strain rate $\|\bar{\boldsymbol{S}}\| = \sqrt{2\bar{S}_{ij}\bar{S}_{ij}}$
which is calculated by the non-equilibrium part of the mean second-order moment $\bar{\boldsymbol{\Pi}}$,

$$\bar{S}_{ij} = -\frac{\bar{\Pi}_{ij}}{2\tau_{total}\rho RT} \tag{13}$$

where $\bar{\Pi}_{ij} = \sum_{\alpha} \boldsymbol{e}_{\alpha i}\boldsymbol{e}_{\alpha j} f_{\alpha} - f_{eq}$ and $\tau_{\mathrm{total}} = \frac{\nu+\nu_t}{\delta t} + \frac{1}{2}$ represents relaxation time in the LBE-LES model. Substituting Eq. 13 into Eq. 12 yields a solution of quadratic equation as,

$$\tau_{total} = \frac{1}{2}\tau + \frac{1}{2}\sqrt{\tau^2 + \frac{2(C_s\delta x)^2}{\rho RT}\|\bar{\boldsymbol{\Pi}}\|} \tag{14}$$

where $\|\bar{\boldsymbol{\Pi}}\| = \sqrt{2\bar{\Pi}_{ij}\bar{\Pi}_{ij}}$.

Wave generating and absorbing methods
The distributed momentum source is used to generate waves. The equivalent source term $\boldsymbol{S}_{\mathrm{g}}$ is,

$$\begin{cases} S_{g,x} = g\big(2\beta(x - x_s)\big)e^{-\beta(x-x_s)^2}\dfrac{D}{\omega}\sin\omega t \\ S_{g,y} = 0 \end{cases} \tag{15}$$

where g is the gravity acceleration and β = 20/W^2 is a coefficient of source width W; x_{s} is the centre of wave generating area; D is distribution source density [4].

Sponge layers are adopted to achieve wave dissipation in the two ends of numerical wave flume. In the sponge area with width L_{s}, the damping force $\boldsymbol{S}_{\mathrm{b}}$ is given as,

$$\boldsymbol{S}_b = -(B_1\boldsymbol{u} + B_2\boldsymbol{u}|\boldsymbol{u}|)\frac{e^{\left|\frac{x-x_0}{L_s}\right|^{n_s}} - 1}{e-1} \tag{16}$$

where B_1, B_2 and n_{s} are empirical coefficient, and x_0 is the starting location of the sponge layer.

Dimensionless quantities in LBM system
Different from standard LBM, the present model uses the non-dimensional system associated with physical system as follows,

$$Ma = \frac{u_c}{\sqrt{RT}} \tag{17}$$

where u_c and $\sqrt{RT}$ are the wave phase velocity (or maximum velocity) and characteristic velocities in physical system. For a specific Mach number we can evaluate $\sqrt{RT}$. And the characteristic length L_0 is chosen as the wave amplitude, Then the kinetic viscosity and gravity in lattice system can be calculated by,

$$\nu = \frac{\nu^*\sqrt{RT}}{RTL_0}, \qquad g = \frac{g^*L_0}{RT} \tag{18}$$

where ν* kinetic viscosity and g* is the gravity acceleration in physical system.

RESULTS

Model validation
To validate the effectiveness of the present free-surface model, the Rider-Kothe single vortex test case [6] has been simulated. In the case, the collision and streaming do not be implemented. A given velocity field according to the following streaming function is used to calculated the equilibrium distribution functions as the simulation solution of each iteration.

$$\psi = \frac{2}{\pi}sin^2\,\pi x \cdot sin^2\,\pi y \cdot cos\frac{\pi t}{T} \tag{19}$$

The flow field will restore to the initial state after one period. So the simulation results can be compared with the analytically filled level VOF to verify the purely advection case in absence of collision and streaming. The initial circle centre is located at (0.5, 0.75) and the wave period T is set as 2 s and 128 or 512 grid points is distributed in the 1m square domain. Relative errors of the two grid resolution are 4.5% and 1.4%, respectively.

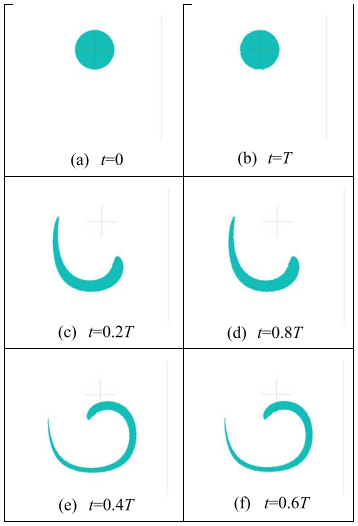

Fig. 2. Evolution of the fluid interface within one period (grid resolution: 512 by 512).

Waves propagating through an OWC

Following the model validation, waves propagating through an OWC without Power take-off system, as shown in Fig. 3, are modelled. In this case, the incident wave amplitude is 0.02m, and water depth h is 0.4m. The wave flume shown in Fig. 1 is used. The wave monitoring locations are also shown in Fig. 3 as WG1 and WG2, before and after the OWC respectively, and WG5 at the location of the OWC. Non-slip boundary condition is implemented in the body surface.

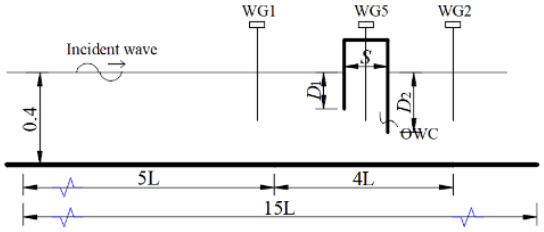

Fig. 3. Schematic diagram for OWC in wave flume.

Fig. 4 shows the wave profiles at t=22T and 26T, along the wave flume. The simulation results in general agree with each other, including the reflected wave in the upstream of the OWC and transmission wave in the downstream end, showing that the numerical stability has been achieved.

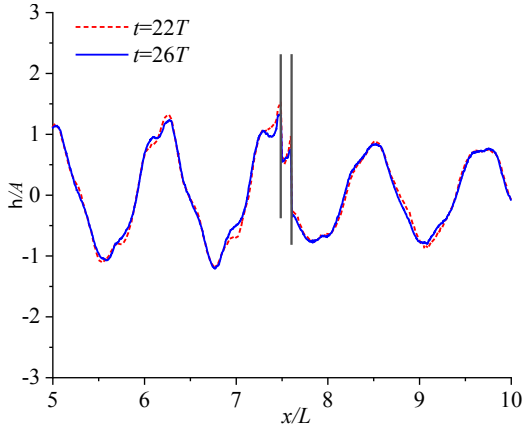

Fig. 4. Water surface elevation η along propagation direction at t=22T and 26T.

In addition, the temporal variations of wave elevation at x=5*L* and 9*L* is presented in Fig. 5, where the potential-flow theoretical solutions are also shown. It is obvious that the maximum amplitude at the seaside is larger than that at the leeside, similar as the linear analytical solution.

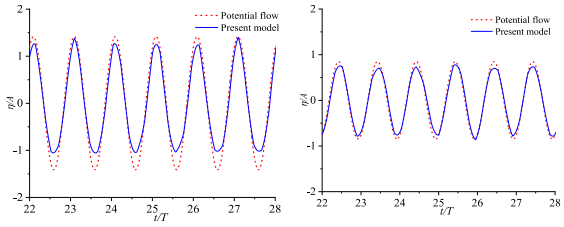

Fig. 5. Water surface elevation η at (a) x=5L (left) and (b) x=9L (right).

For the smaller wave amplitude in the present results, it is attribute to the vortex shedding at the sharp corner below walls and strong nonlinearity, as shown in Fig. 6. Moreover, the stronger nonlinearity in the upstream, due to the larger wave amplitude, causes the more significant discrepancy between linear potential-flow analytical solution and the present numerical results, compared with the transmission wave at the downstream of the OWC.

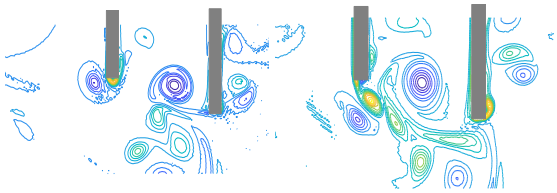

Fig. 6. Vortex contour below wall from the sharp corner (a) $t=t_1$ (left) and (b) $t=t_1+0.19T$ (right).

CONCLUSIONS

In this paper, a free surface model based on VOF-LBM method following [1] is established and is applied to wave-OWC interaction problem. The numerical results show that the present model can simulate complex free surface flow compared with those published works. By imposed momentum sources, the wave generation and absorption functions have been achieved and the numerical stability has been validated. In the wave-OWC interaction, the vortex shedding and strong nonlinearity cause the relatively small amplitude with respect to the linear potential-flow solution.

Acknowledgments

This work was partly supported by the scholarship provided by Cardiff University and China Scholarship Council (No. 202006060048). JM would like to thank the Engineering and Physical Science Research Council under EP/P022243/1 and EP/X035875/1. Thanks also go to the STFC Daresbury Laboratory for hosting the research visit for BG.

Conflicts of interest

The authors declare no conflict of interest.

REFERENCES

[1] C. Janßen and M. Krafczyk, 'Free surface flow simulations on GPGPUs using the LBM', *Computers & Mathematics with Applications*, vol. 61, no. 12, pp. 3549–3563, Jun. 2011. doi.org/10.1016/j.camwa.2011.03.016

[2] G. Liu, J. Zhang, and Q. Zhang, 'A high-performance three-dimensional lattice Boltzmann solver for water waves with free surface capturing', *Coastal Engineering*, vol. 165, p. 103865, Apr. 2021. doi.org/10.1016/j.coastaleng.2021.103865

[3] C. Körner, M. Thies, T. Hofmann, N. Thürey, and U. Rüde, 'Lattice Boltzmann Model for Free Surface Flow for Modeling Foaming', *J Stat Phys*, vol. 121, no. 1–2, pp. 179–196, Oct. 2005. doi.org/10.1007/s10955-005-8879-8

[4] J. Choi and S. B. Yoon, 'Numerical simulations using momentum source wave-maker applied to RANS equation model', *Coastal Engineering*, vol. 56, no. 10, pp. 1043–1060, Oct. 2009. doi.org/10.1016/j.coastaleng.2009.06.009

[5] https://github.com/inmeso/hilemms.

[6] C. Janssen and M. Krafczyk, 'A lattice Boltzmann approach for free-surface-flow simulations on non-uniform block-structured grids', *Computers & Mathematics with Applications*, vol. 59, no. 7, pp. 2215–2235, Apr. 2010. doi.org/10.1016/j.camwa.2009.08.064

Cynhadledd Ymchwil Peirianneg Caerdydd
Cardiff Engineering Research Conference

E. Spezi and M. Bray (eds.) 2024. *Proceedings of the Cardiff University Engineering Research Conference 2023.* Cardiff: Cardiff University Press.
doi.org/10.18573/conf1

Cardiff University Engineering Research Conference 2023 was organised by the School of Engineering and held from 12 to 14 July 2023 at Cardiff University.

The work presented in these proceedings has been peer reviewed and approved by the conference organisers and associated scientific committee to ensure high academic standards have been met.

Cardiff University Press | Gwasg Prifysgol Caerdydd

First published 2024

Cardiff University Press
Cardiff University, PO Box 430
1st Floor, 30-36 Newport Road
Cardiff CF24 0DE

cardiffuniversitypress.org

Editorial design and layout by
Academic Visual Communication

ISBN: 978-1-9116-5349-3 (PDF)